

Group testing for overlapping communities

Pavlos Nikolopoulos*, Sundara Rajan Srinivasavaradhan†, Tao Guo†, Christina Fragouli†, Suhas Diggavi†

*École polytechnique fédérale de Lausanne (EPFL), Switzerland

†University of California Los Angeles (UCLA), USA

Abstract—In this paper, we propose algorithms that leverage a known community structure to make group testing more efficient. We consider a population organized in connected communities: each individual participates in one or more communities, and the infection probability of each individual depends on the communities (s)he participates in. Use cases include students who participate in several classes, and workers who share common spaces. Group testing reduces the number of tests needed to identify the infected individuals by pooling diagnostic samples and testing them together. We show that making testing algorithms aware of the community structure, can significantly reduce the number of tests needed both for adaptive and non-adaptive group testing.

I. INTRODUCTION

A significant challenge to re-open society in the presence of a pandemic is the need for large scale, reliable testing. Group testing is a strategy that can help reduce the number of tests and increase reliability by pooling together diagnostic samples. Accordingly, it is attracting significant attention: several countries (India, Germany, US, China) are currently deploying group testing strategies to help them quickly and reliably identify infected people [1], [2].

In this paper, we build group testing algorithms around an idea “whose time has come”: we propose to leverage a known community structure to make group testing more efficient. Although traditionally the work in group testing assumes “independent” infections, we note that today it is totally feasible to keep track of community structure - several apps are already doing so [3], [4]. Moreover, our approach is well aligned with the need for independent grassroots testing (schools testing their students, companies their workers) where the community structure is explicit (shared classrooms, shared common spaces).

We find that taking into account the community structure can reduce the number of tests we need significantly below the well known combinatorial bound [5], the best we can hope for when not taking this structure into account. Moreover, it enlarges the regime where group testing can offer benefits over individual testing. Indeed, a limitation of group testing is that it does not offer benefits when k grows linearly with n [6], [7]. Taking into account the community structure allows to identify and remove from the population large groups of infected members, thus reducing their proportion and converting a linear to a sparse regime identification. However, we also find that, although our algorithms do not need assume knowledge of the infection probabilities, they do need to correctly know the community structure, and in particular, the community overlaps: not taking into account the overlaps

(assuming communities are disconnected) can deteriorate the performance. Our main contributions include:

- We derive a lower bound on the number of tests, that generalizes the counting bound [5] to overlapping communities.
- We propose a new adaptive algorithm that requires fewer tests than traditional adaptive algorithms to recover the infection status of all individuals without error.
- We propose two nonadaptive algorithms that leverage the community structure to improve reliability over traditional nonadaptive testing. One leverages the structure at the encoder side with a novel test design, while the other one accounts for it at the decoder side with a new decoding algorithm that is based on loopy belief propagation and is generic enough to work on any structure.

The paper is organized as follows: we give known results in Section II, our model in Section III, the lower bound in Section IV, and non-adaptive algorithms in Sections V and VI. Our numerical evaluation is in Section VII.

Note: The proofs of all our theoretical results (in Sections IV–V) can be found in the Appendix of [8], along with an extended explanation of the rationale behind our algorithms.

II. BACKGROUND

Traditional group testing assumes a population of n members out of which some are infected. Two infection models are considered: (i) in the *combinatorial model*, there is a fixed number of infected members k , selected uniformly at random among all sets of size k ; (ii) in the *probabilistic model*, each item is infected independently of all others with probability p , so that the expected number of infected members is $\bar{k} = np$.

A group test τ takes as input samples from n_τ individuals, pools them together and outputs a single value: positive if any one of the samples is infected, and negative if none is infected. More precisely, let $U_i = 1$ when individual i is infected and 0 otherwise. Y_τ takes a binary value calculated as $Y_\tau = \bigvee_{i \in \delta_\tau} U_i$, where \bigvee stands for the OR operator (disjunction) and δ_τ is the group of people participating in the test.

The performance of a group testing algorithm is measured by the number of group tests $T = T(n)$ needed to identify the infected members (for the probabilistic model, the expected number of tests needed). Several setups have been explored in the literature, that include:

- *Adaptive vs. non-adaptive testing:* In adaptive testing, we use the outcome of previous tests to decide what tests to perform next. An example of adaptive testing is *binary splitting*, which implements a form of binary search and is known to be

optimal when the number of infected members is unknown. Non-adaptive testing constructs, in advance, a *test matrix* $\mathbf{G} \in \{0, 1\}^{T \times n}$ where each row corresponds to one test, each column to one member, and the non-zero elements in each row determine the set δ_τ . Although adaptive testing uses less tests than non-adaptive, non-adaptive testing is more practical as all tests can be executed in parallel.

- *Scaling regimes of operation:* assume $k = \Theta(n^\alpha)$, we say we operate in the linear regime if $\alpha = 1$; in the sparse regime if $0 \leq \alpha < 1$; in the very sparse regime if k is constant.

The following are well established performance results (see [5], [9], [10] and references therein):

- Since T tests allow to distinguish among 2^T combinations of test outputs, we need $T \geq \log_2 \binom{n}{k}$ to identify k randomly infected people out of n . This is known as the **counting bound** [5], [9], [10] and implies that we cannot use less than $T = O(k \log \frac{n}{k})$ tests.
- Noiseless adaptive testing allows to achieve the counting bound for $k = \Theta(n^\alpha)$ and $0 \leq \alpha < 1$; for non-adaptive testing, this is also true of $0 \leq \alpha < 0.409$, if we allow a vanishing (with n) error [5], [11], [12].
- In the linear regime ($\alpha = 1$), group testing offers little benefits over individual testing. In particular, if the infection rate k/n is more than 38%, group testing does not use fewer tests than one-to-one (individual) testing unless high identification-error rates are acceptable [6], [7], [13].

III. MODEL AND NOTATION

A. Community model

Our work extends the above results by assuming an overlapping community structure: members may belong to one or more communities—hence they are infected according to new combinatorial and probabilistic models that are slightly different from the traditional ones and depend on how the communities overlap (Section III-B). Given these new infection models, new lower bounds can be derived (Section IV) for both the combinatorial and probabilistic case. Our analysis shows that these bounds can be significantly lower than the above-mentioned counting bounds.

More formally, we assume that all members of the entire population $\mathcal{V} = \{1, 2, \dots, n\}$ are organized in a known structure, which can be perceived in the form of a hypergraph $G(\mathcal{V}, \mathcal{E})$: each vertex $v \in \mathcal{V}$ corresponds to an individual, that we simply call a *member*, and each edge $e \in \mathcal{E}$ indicates which members belong to the same *community*. Since G is a hypergraph, an edge may connect any number of vertices; hence, a member may belong to one or more communities. The number of communities that a member belongs to is called the *degree* of the member. Sometimes, we need to reason about the number of communities in the structure and the community size (i.e. the number of members in a community). Instead of the classic cardinality notation, we use the following for brevity: $|\mathcal{E}| = F$, $|\mathcal{V}_e| = M_e$, and $M_e = M$ in the symmetric case where all communities have the same size.

The hypergraph G may be decomposed into connected components, where each component $C(\mathcal{V}_C, \mathcal{E}_C)$ is

a sub-hypergraph. For component C let D_C contain the nonempty subsets of the standard partition of the hyperedges in \mathcal{E}_C ; in the example of Fig. 1, \mathcal{E}_C consists of 3 hyperedges, and D_C contains 7 disjoint sets.

For each set $d \in D_C$, let \mathcal{V}_d denote the set of members it contains. Because of the partition, all members of \mathcal{V}_d belong to the same community (or set of communities), which we denote with $E(\mathcal{V}_d)$ —hence, they all have the same degree. As described

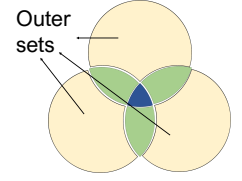


Fig. 1: Example illustrating outer sets.

in the next section, these members get infected according to some common infection principle. We distinguish 2 kinds of sets in D_C : (a) the “outer” sets: $D_{C,out} \triangleq \{d \in D_C : \nexists b \in D_C \text{ s.t. } E(\mathcal{V}_b) \subset E(\mathcal{V}_d)\}$, and (b) the “inner” sets: $D_{C,in} \triangleq D_C \setminus D_{C,out}$. Fig. 1 illustrates the 3 outer (yellow) and 4 inner (green and blue) sets. Note that the members of inner sets have always a higher degree than those of the outer sets.

B. Infection models

Let $K(\text{set})$ return the subset of infected elements of any *set* of members, communities or components. We consider the following infection models, that parallel the ones in the traditional setup of Section II.

- **Combinatorial Model (I).** k_f of the communities have at least one infected member (we will call these *infected communities*). The rest of the communities have no infected members. Any combination of infected communities has the same chance of occurring. In each infected community, there are $k_m^e = |K(\mathcal{V}_e)|$ infected members, out of which $k_m^{\mathcal{J}} = |K(\cap_{e \in \mathcal{J}} \mathcal{V}_e)|$ (with $\cap_{e \in \mathcal{J}} \mathcal{V}_e \neq \emptyset$) are shared with a subset of communities \mathcal{J} . The infected communities (resp. infected community members) are chosen uniformly at random out of all communities (resp. members of the same community).

- **Probabilistic Model (II).** A community e becomes infected i.i.d. with probability q . If a member v of an infected community e belongs *only* to that community (i.e. has degree 1), then it becomes infected w.p. $p_v = p_e$, independently from the other members (and other communities). Also, if v belongs to a subset of infected communities $K(\mathcal{J}) \subseteq K(\mathcal{E})$, it is considered to be infected by either of these communities. So, given all the infection rates of these communities $\{p_e : e \in K(\mathcal{J})\}$, we say that v becomes infected w.p.: $p_v = 1 - \prod_{e \in K(\mathcal{J})} (1 - p_e)$. Note that since each member gets infected by either of the infected communities it belongs to, the product of the RHS term above becomes smaller as $|K(\mathcal{J})|$ increases. Last, if v does not belong to an infected community, then $p_v = 0$.

We make two remarks: First, although the communities are infected independently, their structure causes a dependent infection model; in fact, the way communities overlap determines the infection probability of their shared members. Second, our model captures situations where infection is

determined by participation in a community rather than the status of community members. Albeit simplistic, we think that this model can be useful in real pandemics. Since the exact community structure of the entire population of a country or a continent can never be known to the test designer, we expect that graph G only partially describes the reality: there might be members that do not belong to \mathcal{V} , yet interact with them in unknown ways, or there might be communities that are simply not captured due to unknown member interactions. In such a case, assuming that communities become infected independently seems a simple yet reasonable model to use. However, once a few communities in G get infected, we expect that the infection probability of a member will increase with the number of infected communities it belongs to, which is captured by our model in the computation of p_v .

Non-overlapping communities: A special case of our community framework is when the communities have no overlap; this scenario is investigated in our prior work [14], where algorithms that take into account the non-overlapping structure are explored. In our experiments, however, these algorithms do not always perform well when communities overlap (e.g. see Fig. 3); in fact, there are cases (shown in [8]), where they perform worse than traditional group testing.

IV. LOWER BOUND ON THE NUMBER OF TESTS

We compute the minimum number of tests needed to identify all infected members under the zero-error criterion in both community models (I) and (II).

Theorem 1 (Community bound for combinatorial model (I)). *Any algorithm that identifies all k infected members without error requires a number of tests T satisfying:*

$$T \geq \log_2 \binom{F}{k_f} + \sum_{C \in G} \sum_{d \in D_C} \log_2 \binom{|\mathcal{V}_d|}{|K(\mathcal{V}_d)|}, \quad (1)$$

where $|\mathcal{V}_d|$ is the set of members of each disjoint set in D_C and $|K(\mathcal{V}_d)|$ are the infected members of that set.

Observation: Consider a usual epidemic scenario, where the population is composed of a large number of communities with members that have close contacts (e.g. relatives, work colleagues, students who attend the same classes, etc.). In such a case, one should expect that most members of infected communities are infected (i.e. $k_m^e \approx M_e$), even though the number of infected communities k_f and the overall number of infected members k may still follow a sparse regime (i.e., $k_f = \Theta(F^{\alpha_f})$ and $k = \Theta(n^\alpha)$ for $\alpha_f, \alpha \in [0, 1)$).

Theorem 1 shows the significant benefit of taking the community structure into account in the test design: the community bound increases almost *linearly* with k_f , as opposed to k , which is what happens with the traditional counting bound (that does not account for any community structure). This is due to the second term of Equation (1) tending to 0 and $\log_2 \binom{F}{k_f} \sim k_f \log_2 \frac{F}{k_f} \sim (1 - \alpha_f) k_f \log_2 F$.

A similar bound exists for the probabilistic model (II). Consider a component $C \in G$. Let \mathbf{X}_C be the indicator random vector for the infection stat of all communities in C ,

and $\mathcal{X}_C = \{0, 1\}^{|C|}$ be the set of all possible such indicator vectors. Note that since each community becomes infected w.p. q , $\mathbb{P}(\mathbf{X}_C = \mathbf{x}_C) = q^\lambda (1 - q)^{|C| - \lambda}$, where λ is the weight of \mathbf{x}_C . Also, the value of \mathbf{x}_C determines the infection probabilities p_v of each member $v \in \mathcal{V}_C$.

Theorem 2 (Community bound for probabilistic model (II)). *Any algorithm that identifies all infected members without error requires a number of tests T satisfying:*

$$T \geq F h_2(q) + \sum_{C \in G} \sum_{\mathbf{x}_C \in \mathcal{X}_C} \mathbb{P}(\mathbf{X}_C) \cdot \sum_{v \in \mathcal{V}_C} h_2(p_v | \mathbf{X}_C) \quad (2)$$

where h_2 is the binary entropy function.

Theorem 2 extends from zero-error recovery to constant-probability recovery, if we apply Fano's inequality in a similar way to Thm 1 of [15]: $\mathbb{P}(\text{suc}) \leq T / (h_2(q) + \sum_{C \in G} \sum_{\mathbf{x}_C} \mathbb{P}(\mathbf{X}_C) \cdot \sum_{v \in \mathcal{V}_C} h_2(p_v | \mathbf{X}_C))$.

V. ALGORITHMS

In this section, we provide group-testing algorithms for the noiseless case that leverage the community structure. We start from adaptive algorithms and then proceed to non-adaptive.

Algorithm 1 Adaptive Community Testing ($G(\mathcal{V}, \mathcal{E})$)

\hat{U}_v is the estimated infection state of member v (“+” or “-”).
 \hat{U}_z is the estimated infection state of a mixed sample z .

```

1: for  $d \in D_{C, \text{out}}, \forall C \in G$  do
2:    $r_d \leftarrow \text{SelectRepresentatives}(\mathcal{V}_d)$ 
3: end for
4:  $\{\hat{U}_{z(r_d)}\} \leftarrow \text{AdaptiveTest}(\{z(r_d)\})$ 
5: Set  $A := \emptyset$ 
6: for  $C \in G$  do
7:   for  $d \in D_{C, \text{out}}$  do
8:     if  $\hat{U}_{z(r_d)} = \text{“positive”}$  then
9:       Individually test  $\mathcal{V}_d$ :  $\hat{U}_v \leftarrow U_v, \forall v \in \mathcal{V}_d$ .
10:       $\hat{p}_d \leftarrow 1/|\mathcal{V}_d| \cdot \sum_{v \in \mathcal{V}_d} \mathbf{1}\{\hat{U}_v = \text{‘positive’}\}$ 
11:     else
12:        $A \leftarrow A \cup \{v : v \in \mathcal{V}_d\}$ 
13:     end if
14:   end for
15:   for  $b \in D_{C, \text{in}}$  (in increasing order of degree) do
16:     if  $\exists d \in D_C$  s.t.  $E(\mathcal{V}_d) \subset E(\mathcal{V}_b)$  &  $\hat{p}_d > \theta$  then
17:       Individually test  $\mathcal{V}_b$ :  $\hat{U}_v \leftarrow U_v, \forall v \in \mathcal{V}_b$ .
18:        $\hat{p}_b \leftarrow 1/|\mathcal{V}_b| \cdot \sum_{v \in \mathcal{V}_b} \mathbf{1}\{\hat{U}_v = \text{‘positive’}\}$ 
19:     else
20:        $A \leftarrow A \cup \{v : v \in \mathcal{V}_b\}$ 
21:     end if
22:   end for
23: end for
24:  $\{\hat{U}_v : v \in A\} = \text{AdaptiveTest}(A)$ 
25: return  $[\hat{U}_1, \dots, \hat{U}_n]$ 

```

A. Adaptive algorithm

Algorithm 1 describes our adaptive algorithm. It is built on top of traditional adaptive testing, which we will generally denote as $AdaptiveTest()$. $AdaptiveTest()$ is an abstraction of any existing (or future) adaptive algorithm that assumes independent infections. We distinguish 2 different inputs for $AdaptiveTest()$: (a) a set of members; or (b) a set of *mixed samples*. A mixed sample is created by pooling together samples from multiple members. For example, mixed sample $z(r_d)$ is a pooled sample of some representative members r_d from disjoint set d . Because we only care whether a mixed sample is positive or not, we can treat it in the same way as an individual sample—hence use group testing to identify the state of mixed samples as we do for individuals.

Part 1: For each component of the graph G , we first identify the outer sets $D_{C,out}$. Then, from each outer set d , we select a representative subset of members r_d , whose samples are pooled together into a mixed sample $z(r_d)$. There can be many selection methods for $SelectRepresentatives()$; however, we typically use uniform (random) sampling without replacement. Finally, we determine the state of all mixed samples (line 4).

Part 2: We treat $\hat{U}_{z(r_d)}$ as a rough estimate of the infection regime inside each set d : if $\hat{U}_{z(r_d)}$ is positive, we consider d to be heavily infected and we individually test its members (line 9); otherwise, we consider it lightly infected and we include its members in set A (line 12). For our rough estimate of the infection regime to be a good one, we choose the number of representatives based on some prior information about infection rate of each outer set; for example if $p_e < 38\%$ then only one representative is enough, otherwise pooling together the entire set is one’s best option. Note that the exact knowledge of p_e and a rough prior may be easily acquired. For example, in realistic scenarios, where the infection rates are not expected to be very low inside the communities, pooling together the entire outer set is a good heuristic.

Due to individually testing the heavily-infected outer sets, we obtain more accurate estimates of their infection rates, \hat{p}_d , by computing the average proportion of infected members (line 10). We use these estimates to decide how to test the inner sets of the component: if an outer set d exists whose members belong to a subset of communities in $E(\mathcal{V}_b)$ and its estimated infection rate \hat{p}_d is above a threshold θ , then members of \mathcal{V}_b are tested individually (line 17) and a new estimate \hat{p}_b for the infection rate of that set is computed (line 18). Else, members of \mathcal{V}_b are included in set A . Our rationale follows the infection model described in Section III-B, which implies that the infection probability of the members of an inner set b will always be at least equal to the infection probability of the members (of an outer set d) whose community(ies) are a subset of $E(\mathcal{V}_d)$. Hence, if an outer set is heavily infected then a corresponding inner set will be heavily infected, too. In our experiments, we numerically examine the impact of θ .

Finally, we test all members of set A that are not tested individually (because infection probability is presumably low) using traditional group testing (line 23).

B. Non-adaptive algorithms

For simplicity, we describe our non-adaptive algorithm using the symmetric case.

Test Matrix. We divide the $(T_1 + T_2) \times n$ matrix \mathbf{G} into two sub-matrices \mathbf{G}_1 and \mathbf{G}_2 of sizes $T_1 \times n$ and $T_2 \times n$.

▷ The sub-matrix \mathbf{G}_1 identifies the non-infected outer sets using one mixed sample for each outer set (Section III-A). If the number of tests available is large, we set T_1 to be the number of outer sets, i.e., we use one test for each outer set; otherwise, in sparse k_f regimes, T_1 can be closer to $\mathcal{O}(k_f \log \frac{F}{k_f})$.

▷ Assume that $T_2 = \frac{n}{c}$, for some constant c . The sub-matrix \mathbf{G}_2 of size $T_2 \times n$ has one “1” in each column (each of the n member participates in one test) and c “1”s in each row (each test pools together c members); equivalently, \mathbf{G}_2 is a concatenation of c identity matrices I_{T_2} , i.e., $\mathbf{G}_2 = [I_{T_2} \ I_{T_2} \ \cdots \ I_{T_2}]$. For $c = 1$, this reduces to individual testing. The design of \mathbf{G}_2 amounts to deciding which members are placed in the same test. We propose that no two members from the same outer set are placed in the same test and that members from the same inner set are placed in the same test (c members in each test).

Decoding. We use the test outcomes of \mathbf{G}_1 to identify the non-infected outer sets and proceed to remove the corresponding columns from \mathbf{G}_2 . We next use the remaining columns of \mathbf{G}_2 and combinatorial orthogonal matching pursuit (COMP) to identify the infected members, namely: (i) A member is identified as non-infected if it is included in at least one negative test in \mathbf{G}_2 . (ii) All other members, that are only included in positive tests in \mathbf{G}_2 , are identified as infected.

Intuition. Suppose infected communities have a large percentage (say $> 40\%$) of infected members. The idea is that pooling together multiple highly correlated items in the same test (such as people in the same outer/inner set) enables COMP to mark all these items as non-defective in case of a negative result.

Example. We here illustrate for a special case our proposed design for matrix \mathbf{G}_2 and the resulting error rate our algorithm achieves. Assume that we have F communities, where $2F_o$ communities pairwise overlap (each community overlaps with exactly one other community) and the remaining $F - 2F_o$ communities do not overlap with any other community. Assume each community has M members, and overlapping communities share M_o members. We construct the sub-matrix \mathbf{G}_2 of size $T_2 \times n$ as in the following example that uses $F = 6$, $F_o = 2$, $M = 3$, $M_o = 1$:

$$\mathbf{G}_2 = \begin{bmatrix} I_3 & & & I_3 & & & \\ & I_2 & & & I_2 & & \\ & & I_1 & & & I_1 & \\ & & & I_2 & & & I_2 \end{bmatrix}.$$

This matrix starts with $b_1 = \frac{F-2F_o}{c}$ block-rows that each contains c identity matrices I_M , one corresponding to each non-overlapping community. We then have $b_2 = \frac{F_o}{c}$ block-rows each containing c identity matrices I_{2M-M_o} , one for each pair of overlapping communities. Each I_{2M-M_o} matrix contains three matrices I_{M-M_o} , I_{M_o} , and I_{M-M_o} corresponding to the members that belong only in one of

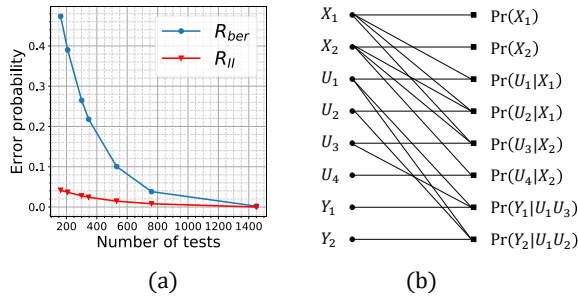


Fig. 2: (a). Error rate for Bernoulli design vs G_1G_2 design for the example. (b). An example of factor graph.

the communities, or in both. Note that $F = (b_1 + 2b_2)c$ and $T_2 = b_1M + b_2(2M - M_o)$.

Error Rate. Note that our decoding strategy leads to zero FN errors. The following lemma provides an analysis of the error (FP) rate for the design of \mathbf{G}_2 in the example which is defined as: $R(\text{error}) \triangleq 1/n \cdot |\{v : \hat{U}_v \neq U_v\}|$. We provide the expected error rate for only the probabilistic model (II) for the purpose of comparison with traditional Bernoulli design in Fig. 2(a).

Lemma 1. For \mathbf{G}_2 as in the example, the error rate is calculated for the probability model (II) as:

$$R_{II}(\text{error}) = \frac{1}{n} \left[(1 - (1 - pq)^{c-1}) \cdot N_1 + (1 - (1 - pq)^{2(c-1)}) \cdot N_2 \right], \quad (3)$$

where N_1 and N_2 are the expected number of non-overlapped and overlapped members in infected communities that are non-infected, respectively, and can be obtained as

$$N_1 = (F - 2F_o)q(1 - p)M + 2F_oq(1 - p)(M - M_o)$$

$$N_2 = F_o(1 - (1 - q)^2)(1 - p)M_o.$$

The error rate of traditional group testing using Bernoulli design (with parameter $\frac{1}{k}$) and COMP decoding has an error rate of $R_{\text{tradition}}(\text{error}) = 1/n \cdot (n - k) (1 - 1/k(1 - 1/k)^k)^T$. Fig. 2(a) depicts $R(\text{error})$ for parameters $F = 150$, $F_o = 60$, $M = 10$, $M_o = 2$, $q = 0.2$, and $p = 0.2$.

VI. LOOPY BELIEF PROPAGATION DECODER

Apart from COMP, we also use loopy belief propagation (LBP [16]) to infer the infection status of the individual (and communities). LBP forms an estimate of the posterior probability that an individual (or a community) is infected, given the test results. This estimate is exact when the underlying factor graph describing the joint distribution is a tree, however this is rarely the case. Nevertheless, it is an algorithm of practical importance and has achieved success on a variety of applications. Also, LBP offers soft information (posterior distributions), which is more useful than hard decisions in the context of disease-spread management.

We use LBP for our probabilistic model, because it is fast and can be easily configured to take into account the community structure. Many inference algorithms exist that estimate the posterior marginals, some of which have also

been employed for group testing. For example, GAMP [17] and Monte-Carlo sampling [18] yield more accurate decoders. However, taking into account the statistical information provided by the community structure is not trivial with more sophisticated decoders such as these. Moreover, the focus of this work is to examine whether benefits from accounting for the community structure (both at the test design and the decoder) exist; hence we think that considering a simple (possibly sub-optimal) decoder based on LBP is a good first step; we defer more complex designs to future work.

We next describe the factor graph and the belief propagation update rules for our probabilistic model (II). Let the infection status of each community e be $X_e \sim \text{Ber}(q)$. Moreover, let S_v denote the set of communities that U_v belongs to. Then:

$$\mathbb{P}(X_1, \dots, X_F, U_1, \dots, U_n, Y_1, \dots, Y_T) = \prod_{e=1}^F \mathbb{P}(X_e) \prod_{v=1}^n \mathbb{P}(U_v | X_{S_v}) \prod_{\tau=1}^T \mathbb{P}(Y_\tau | U_{\delta_\tau}), \quad (4)$$

where δ_τ is the group of people included in test τ . Equation (4) can be represented by a factor graph, where the variable nodes correspond to the variables X_e, U_v, Y_τ and the factor nodes correspond to $\mathbb{P}(X_e), \mathbb{P}(U_v | X_{S_v}), \mathbb{P}(Y_\tau | U_{\delta_\tau})$; Fig. 2(b) shows an example of 2 communities, 4 members and 2 tests.

Given the result of each test is y_τ , i.e., $Y_\tau = y_\tau$, LBP estimates the marginals $\mathbb{P}(X_e = v | Y_1 = y_1, \dots, Y_T = y_T)$ and $\mathbb{P}(U_v = u | Y_1 = y_1, \dots, Y_T = y_T)$, by iteratively exchanging messages across the variable and factor nodes. The messages are viewed as *beliefs* about that variable or distributions (a local estimate of $\mathbb{P}(\text{variable} | \text{observations})$). Since all random variables are binary, each message is a 2-dimensional vector.

We use the factor graph framework from [16] to compute the messages: Variable nodes Y_τ continually transmit the message $[0, 1]$ if $y_\tau = 1$ and $[1, 0]$ if $y_\tau = 0$ on its incident edge, at every iteration. Each other variable node (X_e and U_v) uses the following rule: for incident edge ϵ , the node computes the elementwise product of the messages from every other incident edge and transmits this along ϵ . For the factor node messages, we derive closed-form expressions for the sum-product update rules (akin to equation (6) in [16]). The exact messages are described in the Appendix of the longer version [8].

VII. NUMERICAL EVALUATION

In this section, we evaluate the benefit of accounting for the community structure, in terms of error rate and number of tests required, using 100 random structures, each having $n = 3000$ members participating in about 200 overlapping communities. **Experimental setup.** We generate each structure using the following rules: the size of each community is selected uniformly at random from the range $[15, 25]$, and each member is randomly allocated in at most 4 communities (according to a geometric distribution). Then, the members become infected according to the probabilistic model (II): each community e gets infected w.p. $q = 0.05$; and if infected, then its infection rate p_e is randomly chosen from the interval $[0.3, 0.9]$. We remark that our experimental setup yields a linear infection

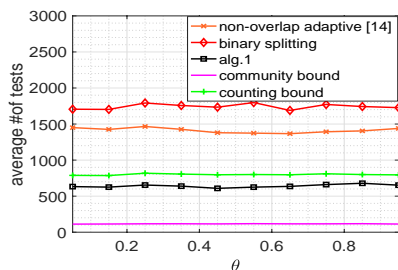


Fig. 3: Average number of tests comparison of various adaptive algorithms and combinatorial bound.

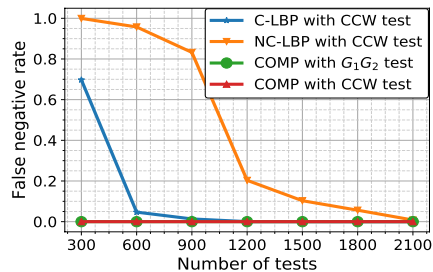


Fig. 4: FN rate comparison of various non-adaptive test designs with corresponding decoding algorithms.

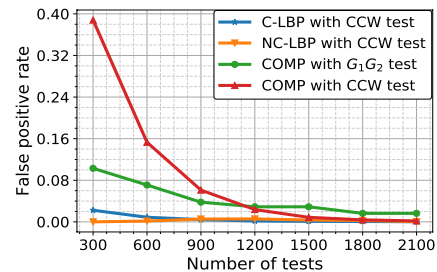


Fig. 5: FP rate comparison of various non-adaptive test designs with corresponding decoding algorithms.

regime; the fraction of infected members about 5% overall. We preferred such a setup in order to stress the performance of our algorithms, as we know that group testing generally shows less benefits in linear regimes.

For the adaptive algorithms, we compare: the binary splitting algorithm (BSA) [5], which is the best traditional alternative when the number of infected members is unknown; the algorithm proposed in [14] that considers communities but no overlap; and Alg. 1 with BSA in the place of *AdaptiveTest()*.

For the non-adaptive test matrix designs, we compare: G_1G_2 , our proposed test design in Section V-B; and *CCW*, constant-column-weight algorithms, where each item is included in a fixed number w of tests selected uniformly at random. w is assumed to be of the form $w = \alpha \frac{T}{k}$, where k is an estimate of the number of defectives in the population. We exhaustively search to find the best value of $\alpha \in [0, 1]$.

We also compare LBP and COMP decoding: *C-LBP* is our proposed algorithm in section VI, that takes into account the community structure. *NC-LBP*, does not take into account the community structure, i.e., assumes that each individual is i.i.d infected with the same probability p_{iid} . *COMP*, described in [5], has a zero FN probability by design.

Results.

(i) *Adaptive test designs.* For each community structure, we measured the number of tests needed by each adaptive algorithm to achieve zero-error identification. Since Alg. 1 depends on θ , the threshold used at line 16, we wanted to evaluate its performance of various values of θ . Figure 3 depicts the average performance of our algorithm (for each θ , we average over 100 randomly generated structures). Alg. 1 was proved resilient to the choice of θ and needed on average $> 60\%$ fewer tests than the other algorithms. Its performance was also better than the counting bound, which is our best hope with traditional group testing. Our findings were similar in sparse infection regimes as well, and there were cases where our algorithm performed close to the community bound [8].

(ii) *Non adaptive test designs.* In our experiments, we measured the FN/FP rates achieved by the non-adaptive test designs and the corresponding decoders. Fig. 4 and Fig. 5 depict FN and FP rates as a function of $T \in [300, 2100]$, respectively. The key takeaways are as follows:

- C-LBP with CCW attains zero FP and FN at 1200 tests

while COMP and NC-LBP with CCW (which are agnostic to the community structure) attain zero FP and FN only at 1800 and 2100 tests respectively. This illustrates potential benefits of making the decoder aware of the community structure.

- If we desire a zero FN rate (or if we would like to use a simple decoder) and we are constrained to use less than 1000 tests, the G_1G_2 test design with COMP gives the lowest FP rates. This illustrates the benefit of designing tests matrices that take into account the community structure.

REFERENCES

- [1] S. Mallapaty, “The mathematical strategy that could transform coronavirus testing,” 2020. [Online]. Available: <https://www.nature.com/articles/d41586-020-02053-6>
- [2] FDA, “Pooled sample testing and screening testing for covid-19,” 2020. [Online]. Available: <https://www.fda.gov/medical-devices/coronavirus-covid-19-and-medical-devices/pooled-sample-testing-and-screening-testing-covid-19>
- [3] “Decentralized privacy-preserving proximity tracing,” *arXiv preprint arXiv:2005.12273*, 2020.
- [4] “Google covid-19 community mobility reports: Anonymization process description (version 1.0),” *arXiv preprint arXiv:2004.04145v2*, 2020.
- [5] M. Aldridge, O. Johnson, and J. Scarlett, “Group testing: an information theory perspective,” *CoRR*, vol. abs/1902.06002, 2019.
- [6] M. C. Hu, F. K. Hwang, and J. K. Wang, “A boundary problem for group testing,” *SIAM Journal on Algebraic Discrete Methods*, 1981.
- [7] P. Ungar, “Cutoff points in group testing,” *Comm. Pure Appl. Math.*, vol. 13, p. 49–54, 1960.
- [8] “Tech. report,” <https://sites.google.com/view/icc-techreport/home>, 2020.
- [9] O. T. Johnson, “Strong converses for group testing from finite block-length results,” *IEEE Trans. Inf. Theory*, 2017.
- [10] D.-Z. Du and F. Hwang, *Combinatorial Group Testing and Its Applications*. Series on Applied Mathematics, 1993.
- [11] A. Coja-Oghlan, O. Gebhard, M. Hahn-Klimroth, and P. Loick, “Information-theoretic and algorithmic thresholds for group testing,” *IEEE Trans. Inf. Theory*, 2020.
- [12] A. Coja-Oghlan, O. Gebhard, M. Hahn-Klimroth, and P. Loick, “Optimal group testing,” ser. Proceedings of Machine Learning Research, J. Abernethy and S. Agarwal, Eds., vol. 125, Jul. 2020, pp. 1374–1388.
- [13] L. Riccio and C. J. Colbourn, “Sharper bounds in adaptive group testing,” *Taiwanese Journal of Mathematics*, p. 669–673, 2000.
- [14] P. Nikolopoulos, T. Guo, C. Fragouli, and S. Diggavi, “Community aware group testing,” *arXiv preprint arXiv:2007.08111*, 2020.
- [15] T. Li, C. L. Chan, W. Huang, T. Kaced, and S. Jaggi, “Group testing with prior statistics,” *CoRR*, vol. abs/1401.3667, 2014.
- [16] F. R. Kschischang, B. J. Frey, and H.-A. Loeliger, “Factor graphs and the sum-product algorithm,” *IEEE Trans. Inf. Theory*, 2001.
- [17] J. Zhu, K. Rivera, and D. Baron, “Noisy pooled pcr for virus testing,” *arXiv preprint arXiv:2004.02689*, 2020.
- [18] M. Cuturi, O. Teboul, and J.-P. Vert, “Noisy adaptive group testing using bayesian sequential experimental design,” *arXiv preprint arXiv:2004.12508*, 2020.

A. Proof of Theorem 1

Proof. Ineq. (1) is because of the following counting argument: There are only 2^T combinations of test results. But, because of the community model I, there are $\binom{F}{k_f} \cdot \prod_{C \in \mathcal{G}} \prod_{d \in D_C} \binom{|\mathcal{V}_d|}{|K(\mathcal{V}_d)|}$ possible sets of infected members that each must give a different set of results. Thus,

$$2^T \geq \binom{F}{k_f} \cdot \prod_{C \in \mathcal{G}} \prod_{d \in D_C} \binom{|\mathcal{V}_d|}{|K(\mathcal{V}_d)|},$$

which reveals the result. The RHS of the latter inequality is because there are $\binom{F}{k_f}$ possible combinations of infected communities, each of which has the same chance of occurring and is associated with a structure of infected components. For each infected component, we consider the standard partition D_C (as in Figure 1). In each disjoint set d of the partition, there are $\binom{|\mathcal{V}_d|}{|K(\mathcal{V}_d)|}$ possible combinations of infected members, each of which having the same chance of occurring—hence the double product of the RHS. Since the binomial coefficient is equal to 1, if the number of infected members in a disjoint set d is 0, instead of focusing only on the infected components and infected disjoint sets, we can let the products at the RHS be over all disjoint sets of all components in the graph. \square

B. Proof of Theorem 2

Proof. Let: U_v be the indicator random variable for the infection status of each member v , \mathbf{U} be the infection-status vector of all members, X_e be the indicator random variable for the infection status of each community e , and \mathbf{X}_C be the infection-status vector of all communities in a connected component C . Also, let $\mathcal{X}_C = \{0, 1\}^{|\mathcal{C}|}$ be the set of all possible such indicator vectors. Since each community becomes infected w.p. q , $\mathbb{P}(\mathbf{X}_C = \mathbf{x}_C) = q^\lambda (1 - q)^{|\mathcal{C}| - \lambda}$, where λ is the weight of \mathbf{x}_C . The value of \mathbf{x}_C determines the infection probabilities p_v of each member $v \in \mathcal{V}_C$.

By rephrasing [15, Theorem 1], any probabilistic group testing algorithm using T noiseless tests can achieve a zero-error reconstruction of \mathbf{U} if:

$$T \geq H(\mathbf{U}) \quad (5)$$

Given the community model II, the joint entropy becomes:

$$\begin{aligned} H(\mathbf{U}) &= \sum_{C \in \mathcal{G}} H(\{U_v : v \in \mathcal{V}_C\}) \\ &= \sum_{C \in \mathcal{G}} H(\mathbf{X}_C) + H(\{U_v : v \in \mathcal{V}_C\} | \mathbf{X}_C) \\ &= \sum_{C \in \mathcal{G}} \sum_{e=1}^{|\mathcal{C}|} h_2(q) + \sum_{\mathbf{x}_C \in \mathcal{X}_C} \mathbb{P}(\mathbf{X}_C) \cdot \sum_{v \in \mathcal{V}_C} h_2(p_v | \mathbf{X}_C) \\ &= F h_2(q) + \sum_{C \in \mathcal{G}} \sum_{\mathbf{x}_C \in \mathcal{X}_C} \mathbb{P}(\mathbf{X}_C) \cdot \sum_{v \in \mathcal{V}_C} h_2(p_v | \mathbf{X}_C) \end{aligned}$$

\square

C. Proof of Lemma 1

For a non-overlapped non-infected member v that belongs to only one community, the probability that v is misidentified as infected is $1 - (1 - pq)^{c-1}$. For an overlapped non-infected member v that belongs to more than one communities, the probability that v is misidentified as infected is $1 - (1 - pq)^{2(c-1)}$. Note that we assume the decoding of \mathbf{G}_1 has no errors, i.e., it identifies all non-infected outer sets correctly. Then for the pairwise overlap structure in the example, the infection status of all non-overlapped communities and non-overlapped parts are identified correctly. The COMP decoding of \mathbf{G}_2 has no FNs. The expected total number of FPs N_0 can be obtained as $N_0 \leq (1 - (1 - pq)^{c-1}) \cdot N_1 + (1 - (1 - pq)^{2(c-1)}) \cdot N_2$, where the inequality is because the RHS have not used the testing results of \mathbf{G}_1 , N_1 and N_2 are the expected number of non-overlapped and overlapped members in infected communities, respectively. We can calculate N_1 as follows,

$$N_1 = (F - 2F_o)q(1 - p)M + 2F_oq(1 - p)(M - M_o), \quad (6)$$

where $(F - 2F_o)q$ is the expected number of infected non-overlapped communities, $(1 - p)M$ is the expected number of non-infected members in each infected non-overlapped community, $2F_oq$ is the expected number of infected overlapped communities, and $(1 - p)(M - M_o)$ is the expected number of non-infected members in each infected overlapped community. Similarly, N_2 can be calculated as

$$N_2 = F_o(1 - (1 - q)^2)(1 - p)M_o, \quad (7)$$

where $F_o(1 - (1 - q)^2)$ is the expected number of overlaps, and $(1 - p)M_o$ is the expected number of non-infected members in each overlapped part.

D. LBP: message passing rules

We here describe our loopy belief propagation algorithm (LBP) and update rules for our probabilistic model (II). We use the factor graph framework of [16] and derive closed-form expressions for the sum-product update rules (see equations (5) and (6) in [16]).

The LBP algorithm on a factor graph iteratively exchanges messages across the variable and factor nodes. The messages to and from a variable node X_e or U_v are *beliefs* about the variable or distributions (a local estimate of $\mathbb{P}(X_e | \text{observations})$ or $\mathbb{P}(U_v | \text{observations})$). Since all the random variables are binary, in our case each message would be a 2-dimensional vector $[a, b]$ where $a, b \geq 0$. Suppose the result of each test is y_t , i.e., $Y_t = y_t$ and we wish to compute the marginals $\mathbb{P}(X_e = x | Y_1 = y_1, Y_2 = y_2, \dots, Y_T = y_T)$ and $\mathbb{P}(U_v = u | Y_1 = y_1, Y_2 = y_2, \dots, Y_T = y_T)$ for $x, u \in \{0, 1\}$. The LBP algorithm proceeds as follows:

- 1) *Initialization:* The variable nodes X_e and U_v transmit the message $[0.5, 0.5]$ on each of their incident edges. Each variable node Y_τ transmits the message $[1 - y_\tau, y_\tau]$, where y_τ is the observed test result, on its incident edge.
- 2) *Factor node messages:* Each factor node receives the messages from the neighboring variable nodes and computes

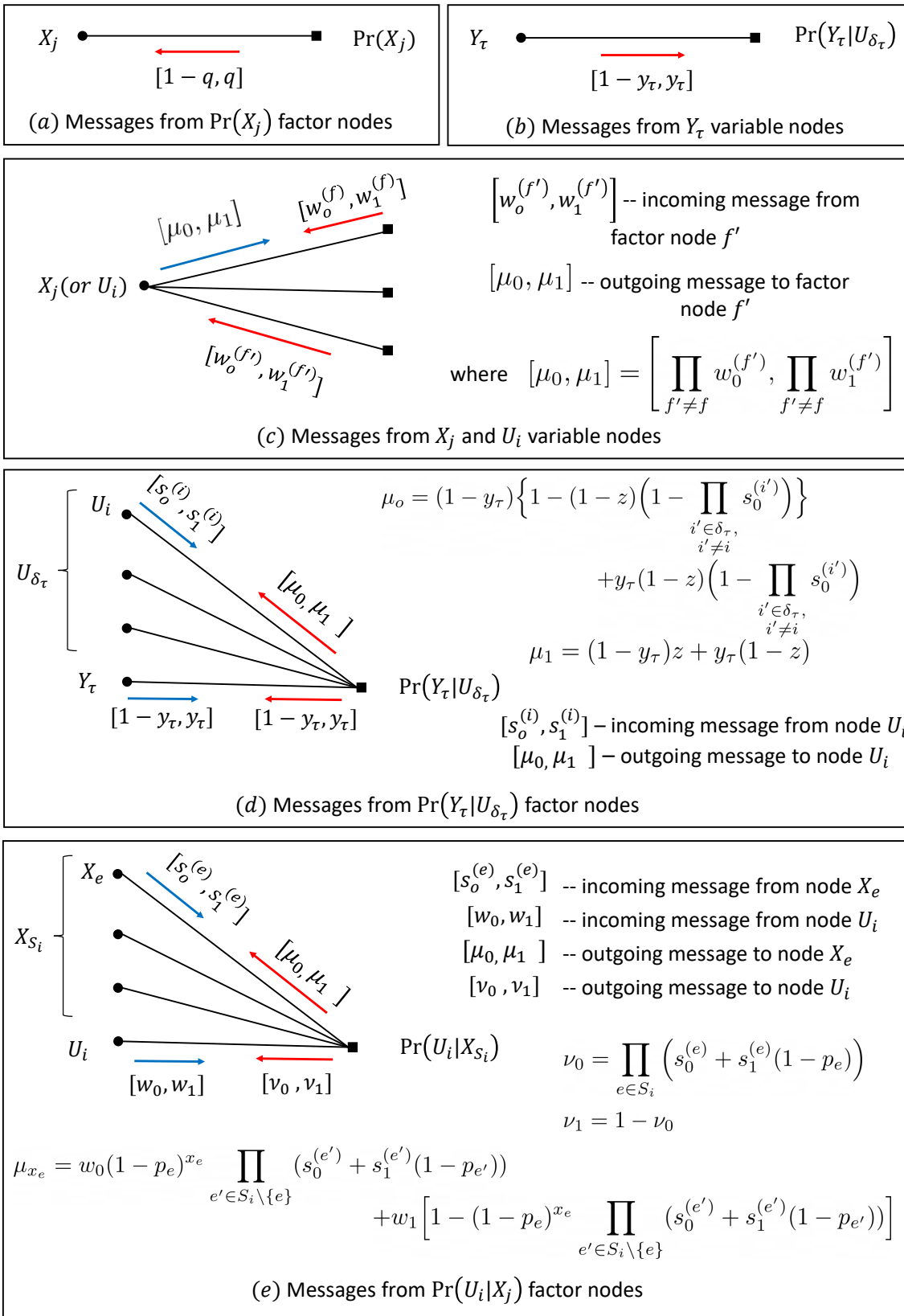


Fig. 6: The update rules for the factor and variable node messages.

a new set of messages to send on each incident edge. The rules on how to compute these messages are described next.

- 3) *Iteration and completion.* The algorithm alternates between steps 2 and 3 above a fixed number of times (in practice 10 or 20 times works well) and computes an estimate of the posterior marginals as follows – for each variable node X_e and U_v , we take the coordinatewise product of the incoming factor messages and normalize to obtain an estimate of $\mathbb{P}(X_e = x|y_1\dots y_T)$ and $\mathbb{P}(U_v = u|y_1\dots y_T)$ for $x, u \in \{0, 1\}$.

Next we describe the simplified variable and factor node message update rules. We use equations (5) and (6) of [16] to compute the messages.

Leaf node messages: At every iteration, the variable node Y_τ continually transmits the message $[0, 1]$ if $Y_\tau = 1$ and $[1, 0]$ if $Y_\tau = 0$ on its incident edge. The factor node $\mathbb{P}(X_e)$ continually transmits $[1 - q, q]$ on its incident edge; see Fig. 6 (a) and (b).

Variable node messages: The other variable nodes X_e and U_v use the following rule to transmit messages along the incident edges: for incident each edge e , a variable node takes the elementwise product of the messages from every other incident edge e' and transmits this along e ; see Fig. 6 (c).

Factor node messages: For the factor node messages, we calculate closed form expressions for the sum-product update rule (equation (6) in [16]). The simplified expressions are summarized in Fig. 6 (d) and (e). Next we briefly describe these calculations.

Firstly, we note that each message represents a probability distribution. One could, without loss of generality, normalize each message before transmission. Therefore, we assume that each message $\mu = [a, b]$ is such that $a + b = 1$. Now, the the leaf nodes labeled $\mathbb{P}(V_j)$ perennially transmit the prior distribution corresponding to V_j .

Next, consider the factor node $\mathbb{P}(U_i|X_{S_i})$ as shown in Fig. 6 (e). The message sent to U_i is calculated as

$$\begin{aligned} \nu_0 &= \sum_{\{x_e \in \{0,1\}: e \in S_i\}} \mathbb{P}(U_i = 0|X_{S_i} = x_{S_i}) \prod_{e \in S_i} s_{x_e}^{(e)} \\ &= \sum_{\{x_e \in \{0,1\}: e \in S_i\}} \prod_{e \in S_i} (s_{x_e}^{(e)} (1 - p_e)^{x_e}) \\ &= \prod_{e \in S_i} (s_0^{(e)} + s_1^{(e)} (1 - p_e)). \end{aligned}$$

Similarly, ν_1 can be computed to be $\nu_1 = 1 - \nu_0$. Now, the message sent to each X_e is

$$\begin{aligned} \mu_{x_e} &= \sum_{\substack{u \in \{0,1\}, \\ \{x_{e'} \in \{0,1\}: e' \in S_i \setminus \{e\}\}}} \mathbb{P}(U_i = u|X_{S_i} = x_{S_i}) w_u \prod_{e' \in S_i \setminus \{e\}} s_{x_{e'}}^{(e')} \\ &= \sum_{\{x_{e'} \in \{0,1\}: e' \in S_i \setminus \{e\}\}} \left(\prod_{e' \in S_i \setminus \{e\}} s_{x_{e'}}^{(e')} \right) \left(w_0 \prod_{e' \in S_i} (1 - p_{e'})^{x_{e'}} \right. \\ &\quad \left. + w_1 (1 - \prod_{e' \in S_i} (1 - p_{e'})^{x_{e'}}) \right) \end{aligned}$$

$$\begin{aligned} &= w_0 (1 - p_e)^{x_e} \prod_{e' \neq e} (s_0^{(e')} + s_1^{(e')} (1 - p_{e'})) \\ &\quad + w_1 \left[1 - (1 - p_e)^{x_e} \prod_{e' \neq e} (s_0^{(e')} + s_1^{(e')} (1 - p_{e'})) \right]. \end{aligned}$$

Finally for the factor nodes $\mathbb{P}(Y_\tau|U_{\delta_\tau})$ as shown in Fig. 6 (d), note that the messages to Y_τ play no role since they are never used to recompute the variable messages. The messages to U_i nodes are expressed as

$$\begin{aligned} \mu_u &= \sum_{\substack{y \in \{0,1\}, \\ \{u_{i'} \in \{0,1\}: i' \in \delta_\tau \setminus \{i\}\}}} \left(\mathbb{P}(Y_\tau = y|U_{\delta_\tau} = u_{\delta_\tau}) \right. \\ &\quad \left. (1 - y_\tau)^{1-y} y_\tau^y \prod_{i' \in \delta_\tau \setminus \{i\}} s_{u_{i'}}^{(i')} \right) \\ &= (1 - y_\tau) \sum_{\substack{\{u_{i'} \in \{0,1\}: \\ i' \in \delta_\tau \setminus \{i\}\}}} \left(\mathbb{P}(Y_\tau = 0|U_{\delta_\tau} = u_{\delta_\tau}) \right. \\ &\quad \left. \prod_{i' \in \delta_\tau \setminus \{i\}} s_{u_{i'}}^{(i')} \right) \\ &\quad + y_\tau \sum_{\substack{\{u_{i'} \in \{0,1\}: \\ i' \in \delta_\tau \setminus \{i\}\}}} \left(\mathbb{P}(Y_\tau = 1|U_{\delta_\tau} = u_{\delta_\tau}) \prod_{i' \in \delta_\tau \setminus \{i\}} s_{u_{i'}}^{(i')} \right). \end{aligned}$$

From our Z-channel model, recall that $\mathbb{P}(Y_\tau = 0|U_{\delta_\tau} = u_{\delta_\tau}) = 1$ if $u_i = 0 \forall i \in \delta_\tau$ and $\mathbb{P}(Y_\tau = 0|U_{\delta_\tau} = u_{\delta_\tau}) = z$ otherwise. Thus we split the summation terms into 2 cases – one where $u_{i'} = 0$ for all i' and the other its complement. Also combining this with the assumption that the messages are normalized, i.e., $s_0^{(i)} + s_1^{(i)} = 1$, we get

$$\begin{aligned} &\sum_{\substack{\{u_{i'} \in \{0,1\}: \\ i' \in \delta_\tau \setminus \{i\}\}}} \left(\mathbb{P}(Y_\tau = 0|U_{\delta_\tau} = u_{\delta_\tau}) \prod_{i' \in \delta_\tau \setminus \{i\}} s_{u_{i'}}^{(i')} \right) \\ &= \mathbb{1}_{u=1} z + \mathbb{1}_{u=0} \left\{ 1 - (1 - z) \left(1 - \prod_{\substack{i' \in \delta_\tau \\ i' \neq i}} s_0^{(i')} \right) \right\}, \end{aligned}$$

and

$$\begin{aligned} &\sum_{\substack{\{u_{i'} \in \{0,1\}: \\ i' \in \delta_\tau \setminus \{i\}\}}} \left(\mathbb{P}(Y_\tau = 1|U_{\delta_\tau} = u_{\delta_\tau}) \prod_{i' \in \delta_\tau \setminus \{i\}} s_{u_{i'}}^{(i')} \right) \\ &= \mathbb{1}_{u=1} (1 - z) + \mathbb{1}_{u=0} \left((1 - z) \left(1 - \prod_{\substack{i' \in \delta_\tau \\ i' \neq i}} s_0^{(i')} \right) \right). \end{aligned}$$

Substituting $u = 0$, and $u = 1$ we obtain the messages

$$\begin{aligned} \mu_0 &= (1 - y_\tau) \left\{ 1 - (1 - z) \left(1 - \prod_{\substack{i' \in \delta_\tau \\ i' \neq i}} s_0^{(i')} \right) \right\} \\ &\quad + y_\tau (1 - z) \left(1 - \prod_{\substack{i' \in \delta_\tau \\ i' \neq i}} s_0^{(i')} \right), \end{aligned}$$

and

$$\mu_1 = (1 - y_\tau) z + y_\tau (1 - z).$$

For our probabilistic model, the complexity of computing the factor node messages increases only linearly with the factor node degree.